DALTON
FULL PAPER

Reactivity of phosphonodithioato Ni^{II} complexes: solution equilibria, solid state studies and theoretical calculations on the adduct formation with some pyridine derivatives †

M. Carla Aragoni,[a] Massimiliano Arca,[a] Francesco Demartin,[b] Francesco A. Devillanova,[a] Claudia Graiff,[c] Francesco Isaia,[a] Vito Lippolis,[a] Antonio Tiripicchio[c] and Gaetano Verani*[a]

[a] *Dipartimento di Chimica Inorganica ed Analitica, Cittadella Universitaria, S.P. per Sestu Km 0.700, 09042, Monserrato, Cagliari, Italy. E-mail: verani@unica.it*
[b] *Dipartimento di Chimica Strutturale e Stereochimica Inorganica e Centro CNR, Via G. Venezian 21, 20133 Milano, Italy*
[c] *Dipartimento di Chimica Generale ed Inorganica, Chimica Analitica, Chimica Fisica, University of Parma, Centro di Studio per la Strutturistica Diffratometrica del CNR, Parco Area delle Scienze 17A, 43100 Parma, Italy*

Received 29th January 2001, Accepted 5th June 2001
First published as an Advance Article on the web 29th August 2001

The reaction between *trans*-bis[*O*-methyl-(4-methoxyphenyl)phosphonodithioato]nickel (**6**) and pyridine (**I**), and *o*-, *m*-, and *p*-aminopyridines (**II–IV**) leads to the 1 : 2 adducts **7**–**10**. The corresponding formation constants have been determined by UV-visible spectroscopy. DFT calculations performed on the free **I–IV** ligands, and EHT-FMO calculations on their interactions with **6** predict an increase in the donor ability on passing from **I** to **IV**. The formation equilibrium constants follow the expected trend [log β_{eq} = 3.20, (**7**); 3.46, (**9**); 4.71 (**10**)], except for **8**, which exhibits the lowest constant (log β_{eq} = 1.88), possibly due to steric effects. The adducts have also been obtained in the solid state, again with the exception of **8**, and compounds **7** and **10** have been characterised by single crystal X-ray diffraction.

Introduction

Dithiophosphorous ligands of the type $RR'PS_2^-$, such as phosphoro- (**1**),[1] phosphono- (**2**) and phosphino-dithioates (**3**, see Scheme 1),[2] and their metal complexes are widely used as

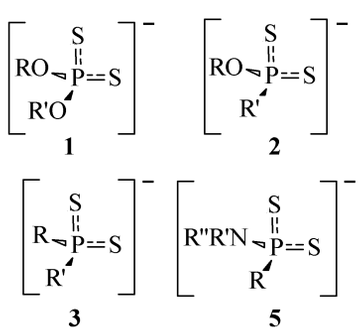

Scheme 1

additives to lubricant oils,[3] antioxidant agents,[4] extraction reagents for metals,[5,6] flotation agents for mineral ores,[5] insecticides, rodenticides, and pesticides.[7] Furthermore, during the past decades, phosphonate derivatives have become very important in replacing the phosphate moiety in biologically active molecules.[8] Although many papers and patents have dealt with the chemistry of ligands of type **1** and **3**,[1,2,5,9] only a few have dealt with those of type **2**, probably because of synthetic difficulties.[10] Recently, following a new reaction path which exploits 1,3-dithia-2,4-diphosphetane-2,4-disulfide derivatives, including the most known Lawesson's reagent (**4**), we have prepared several metal complexes with ligands of type **2** and some amidophosphonodithioate analogues (**5**) with metal ions belonging to Group 10.[11] Square-planar Ni^{II} complexes with ligands of type **1** and **3**, where the metal ion is coordinatively unsaturated, form adducts with donor molecules;[12] this accounts for the significant influence of neutral nitrogen donors on the tribological properties of these complexes when both are present in lubricant oil.[13] Notwithstanding the considerable attention that the adducts with neutral molecules have received,[12] to our knowledge no attempts have been made to investigate the adduct formation equilibria. Even more surprisingly, the reactivity of phosphonodithioate complexes towards neutral donors in the formation of adducts has never been studied at all. Among the previously synthesised square-planar phosphonodithioato complexes,[11] *trans*-bis[*O*-methyl-(4-methoxyphenyl)phosphonodithioato]nickel {[Ni(pdt)$_2$], **6**} has been chosen as a model to study the reactivity of this class of metal complexes towards some pyridine derivatives. We report here the adduct formation equilibria between **6** and pyridine (**I**) and *o*- (**II**), *m*- (**III**), and *p*-aminopyridines (**IV**), together with the syntheses and characterisation of the compounds in the solid state. Furthermore, the interaction between **6** and **I–IV** has been elucidated on the basis of EHT and Hybrid-DFT calculations.

Results and discussion

In order to study the reactivity of Ni^{II} phosphonodithioato complexes towards nitrogen donors, we have chosen *trans*-bis[*O*-methyl-(4-methoxyphenyl)phosphonodithioato]nickel {[Ni(pdt)$_2$], **6**}, synthesised by direct reaction between Lawesson's reagent (**4**) and $NiCl_2$ in methyl alcohol.[11] The addition of a CH_3OH solution of a pyridine derivative **L** [**I**: py; **II**: *o*-NH_2py; **III**: *m*-NH_2py; **IV**: *p*-NH_2py] to a CH_2Cl_2 solution of **6** changes the features of its UV-visible spectrum, and two

† Electronic supplementary information (ESI) available: titration experimental details, UV-visible spectra and calculated data for the formation equilibria of adducts **7**–**10**. See http://www.rsc.org/suppdata/dt/b1/b100991p/

Table 1 Saturation fraction s,[a] adduct formation equilibrium constants β_{eq} (CH_2Cl_2/CH_3OH; T = 25 °C) with their respective errors, peak positions λ_{max} (nm) with molar extinction coefficients ε_{max} (cm^{-1} M^{-1}) in parentheses, and isosbestic points (nm), for compounds **7**–**10**; and ionisation constants[b] (pK) for the free ligands **I**–**IV**

	s[a]	log β_{eq}	λ_{max} (ε_{max})	isosbestic points	pK[b]
6	—	—	536 (110), 694 (100)	—	—
7	0.92	3.20 ± 0.02	454 (188), 718 (94)	494, 718	5.24
8	0.88	1.88 ± 0.02	462 (204), 726 (96)	510, 718	6.71
9	0.97	3.46 ± 0.01	454 (225), 726 (101)	438, 502, 718	6.11
10	0.90	4.71 ± 0.01	454 (227), 734 (109)	438, 502, 710	9.04

[a] Saturation fraction defined as the ratio between the concentration of the formed adduct and the analytical concentration of **6**, calculated at the end of the titration. [b] The pK values refer to the first deprotonation constant of $\mathbf{LH}^+$ (**L** = **I**–**IV**; H_2O, 0.1 M KNO_3, T = 25 °C).

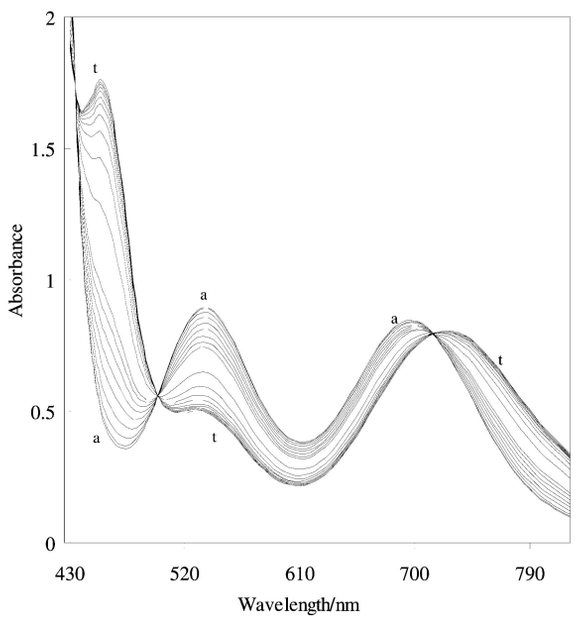

Fig. 1 UV-visible spectra collected during the titration of **6** with **III**. [**III**]/[**6**] = (a): 0; (b): 0.26; (c): 0.51; (d): 0.77; (e): 1.04; (f): 1.28; (g): 1.54; (h): 1.79; (i): 2.05; (j): 3.33; (k): 4.61; (l): 5.89; (m): 7.17; (n): 8.44; (o): 9.72; (p): 11.00; (q): 12.28; (r): 13.56; (s): 14.84; (t): 17.40. Each spectrum has been numerically corrected for dilution. Only the first and last spectra have been labelled for clarity.

bands around 456 and 726 nm take the place of those of **6** falling at 536 and 694 nm. The spectrophotometric titration results obtained for **6** with **III** are shown in Fig. 1. For all the titrations,† the presence of well-defined isosbestic points (see Fig. 1 and Table 1) indicates that only two species are involved in the reaction. The initial spectrum changes on adding increasing amounts of **L**, and tends to assume a different final shape for high [**L**] : [**6**] molar ratios. Fig. 2(a) shows the trend of the absorbance at 454 nm for the case of **III**. The spectra of the solutions recorded at the end of the titrations show very similar features (see Table 1) suggesting that all the pyridine derivatives give similar coordination compounds. The set of spectra recorded for each titration has been analysed using the program SPECFIT,[14] which first calculates both the concentration profiles and the spectra of all the absorbing species by Evolving Factor Analysis (EFA) without any model assumption, and then performs a least-squares optimisation based on an equilibrium model. In all four cases the factor analysis (see Experimental section) confirms that only two absorbing species are involved in the reaction; consequently, besides the free **6**, the second species must be either the 1 : 1 or the 1 : 2 **6** : **L** adduct. The collected data fit well only with the formation of a 1 : 2 adduct, according to equilibrium (1):

$$\underset{\mathbf{6}}{[Ni(pdt)_2]} + 2\underset{\mathbf{I–IV}}{\mathbf{L}} \rightleftharpoons \underset{\mathbf{7–10}}{[Ni(pdt)_2\mathbf{L}_2]} \quad (1)$$

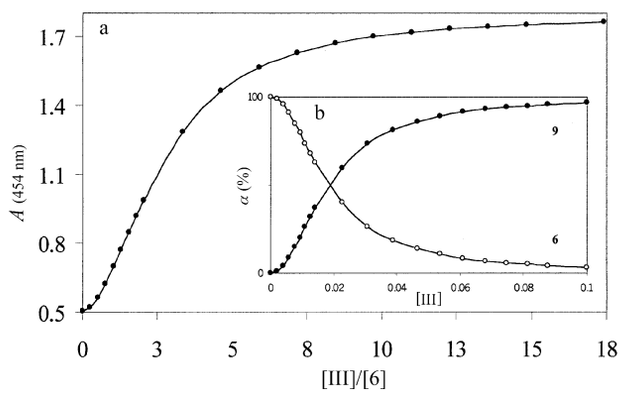

Fig. 2 (a) Plot of absorbance values taken at 454 nm *vs.* the [**III**]/[**6**] molar ratio; (b) distribution curves for the same titration: percentage fractions of **6** and **9** as a function of the concentration of **III**.

In Fig. 2(b) the distribution curves calculated for the formation equilibria of adduct **9** are reported. The adduct formation constants β_{eq} (Table 1) show that the donor ability for all the pyridine derivatives follows the same trend as that outlined by the corresponding ionisation constants,[15] with the exception of **8** which shows the smallest value in the series. This could be ascribed to the steric hindrance of the amino group in the *ortho* position with respect to the endocyclic nitrogen directly involved in the formation of the coordination bond (see below).

The donor ability of pyridine and its derivatives towards the coordinatively unsaturated Ni ion in **6** has been investigated also in the solid state. By evaporating the mixture obtained by adding CH_3OH solutions of the donors **I**, **III**, and **IV** to a CH_2Cl_2 solution of **6** (see Experimental section), we achieved the corresponding adducts $[Ni(pdt)_2\mathbf{L}_2]$, **7**, **9** and **10**, in the solid state. On the contrary, notwithstanding our numerous attempts, we failed to obtain the adduct **8** by reaction of **6** and **II** in the solid state, probably because of its low formation constant due to the above-mentioned hindrance. Analogous steric impediment was invoked in the case of the missed formation of adducts between 2-picoline and Ni^{II} complexes with ligands of type **1**.[12h] Among the three obtained adducts, compound **9** exhibits a noteworthy instability and cannot be isolated from solution because it promptly decomposes by losing donor **III** on standing in open and/or inert atmosphere. In contrast, stable crystals of **7** and **10** suitable for an X-ray crystal structure determination were obtained by slow evaporation of the CH_2Cl_2/CH_3OH reaction mixtures. Fig. 3 and 4 show the structures and labelling schemes for **7** and **10**, and Table 2 reports some selected bond lengths and angles together with those determined for the previously characterised *trans*-bis-[*O*-ethyl-(4-methoxyphenyl)phosphonodithioato]nickel (**11**).[11a] In adduct **7** the central Ni ion displays a pseudo-octahedral environment, with two phosphonodithioate units acting as bidentate ligands and two pyridine molecules axially coordinated to the metal ion through their endocyclic N atoms. The formation of the bis-pyridine adduct causes an increase in the

Table 2 Selected bond lengths (Å) and angles (°) for compounds **7** and **10**. The corresponding values for **11** are reported for comparison

	7	10	11		7	10	11
Ni–N(1)	2.125(3)	2.103(3)	—	N(1)–Ni–N(1)′	180.0	180.00(1)	—
Ni–S(1)	2.504(1)	2.492(1)	2.2197(8)	N(1)–Ni–S(1)	90.90(8)	90.76(9)	—
Ni–S(2)	2.494(1)	2.516(1)	2.2225(8)	S(1)–Ni–S(2)	81.68(4)	81.88(3)	88.14(3)
S(1)–P(1)	1.987(1)	2.000(1)	2.001(1)	S(1)–Ni–S(1)′	180.0	180.0	180.0
S(2)–P(1)	1.998(1)	1.985(1)	1.987(1)	P(1)–S(1)–Ni	84.02(5)	83.74(4)	83.65(3)
P(1)–O(1)	1.598(3)	1.605(2)	1.580(2)	O(1)–P(1)–C(1)	99.1(2)	98.3(1)	99.8(1)
P(1)–C(1)	1.796(3)	1.791(4)	1.782(3)	O(1)–P(1)–S(1)	113.2(1)	110.0(1)	113.4(1)
O(1)–C(8)	1.435(5)	1.432(5)	1.456(4)	C(1)–P(1)–S(1)	111.8(1)	112.2(1)	114.23(9)
				S(1)–P(1)–S(2)	110.19(6)	110.91(5)	101.57(4)
				C(9)–N(1)–Ni	122.7(2)	121.4(2)	—

′ = $-x, -y, -z$.

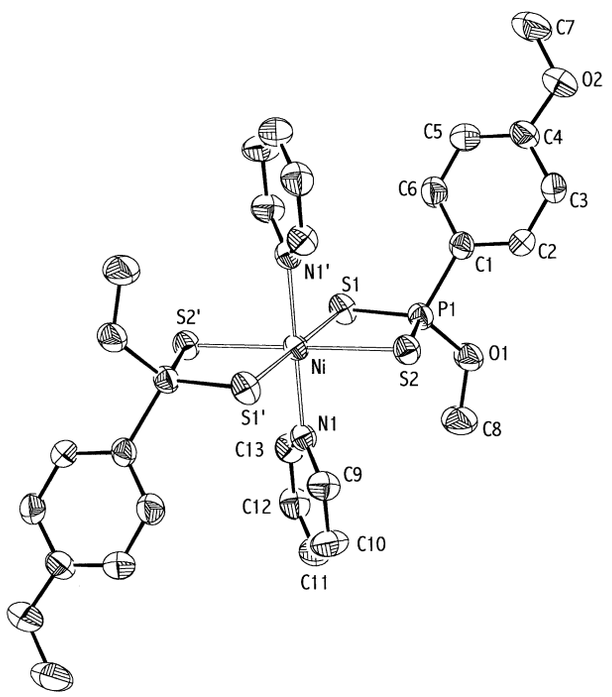

Fig. 3 ORTEP drawing and atom-labelling scheme for compound **7**; hydrogen atoms are omitted for clarity.

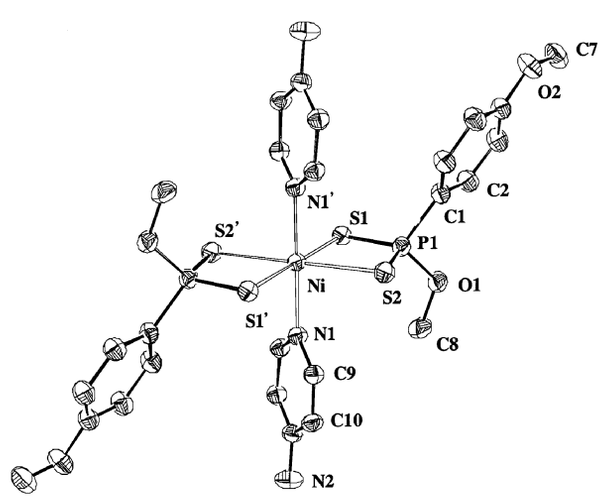

Fig. 4 ORTEP drawing and atom-labelling scheme for compound **10**; hydrogen atoms are omitted for clarity.

Ni–S bond lengths [2.2197(8), 2.2225(8); 2.504(1), 2.494(1) Å for **11** and **7**, respectively] in the phosphonodithioate ligands, and significant variations in the bond angles in the chelate ring. In particular, the angle S(1)–Ni–S(2) decreases from 88.14(3) to 81.68(4)° and the angle S(1)–P–S(2) increases from 101.57(4) to 110.19(6)° on passing from **11** to **7**. The bond lengths and angles in the rest of the phosphonodithioato ligands remain almost unaffected. These variations can be compared with those found in analogous adducts between phosphorodithioato Ni^{II} complexes and pyridine derivatives (Table 3), which were interpreted on the basis of a simple electrostatic model.[12i,16] The coordination of the neutral donor reduces the net positive charge on the central Ni, thus increasing the Ni–S distance and decreasing the S(1)–Ni–S(2) angle; simultaneously, the adduct formation increases the net negative charge on the sulfur atoms and consequently the S–P–S angle.[12i,16] Electron-releasing groups bound to the pyridine ring in positions *ortho* and *para*, which are able to increase the donor properties of the endocyclic N atom, strengthen the coordination bond between the metal ion and the ligand, thus enhancing the mentioned effects. Accordingly, on passing from **7** to **10**, a further shortening of the Ni–N distance [from 2.125(3) in **7** to 2.103(3) Å in **10**] together with a small enlargement of the S(1)–P–S(2) angle [from 110.19(6) to 110.91(5)°] is observed, while the Ni–S bond lengths [2.492(1), 2.516(1) Å] and the S(1)–Ni–S(2) angle [81.88(3)°] in **10** are only slightly different from those of **7**. The bond distances and angles of the nitrogen bases in the adducts remain almost unaltered with respect to the free donors.[17]

A comparison of the FT-IR and FT-Raman spectra of **6**, **7**, and **10** shows very close frequencies for the antisymmetric Ni–S stretching (IR bands at 351, 349, 349 cm^{-1} for **6**, **7**, and **10** respectively), and a slight decrease for the corresponding symmetric vibrations (Raman peaks at 314, 313, 295 cm^{-1}) accompanied by a small increase in the frequencies corresponding to the S(1)–Ni–S(2) bending mode (435, 437, 441 cm^{-1}).

With the aim of better investigating the nature of the interactions between the pyridine derivatives **I–IV** and the complex **6**, we undertook a qualitative interpretation based on the fragment molecular orbital approach (FMO)[18] within extended Hückel formalism (EHT).[19] In **6**, the HOMO is a π-orbital due to the interaction between the four sulfur $3p_z$ and the $3d_{xz}$ and $3d_{yz}$ atomic orbitals (ao's) of the metal ion (see Fig. 5). The LUMO is a σ-antibonding combination between the $3d_{x^2-y^2}$ Ni ao with the four sulfur 3p ao's pointing to the nickel centre. The interaction of the square-planar phosphonodithioato complex with the pyridine molecules does not directly involve these two molecular orbitals: on the contrary, DFT calculations performed on the free ligand **I** show that the centrosymmetric a_g combination of the HOMO's of the two pyridine units (a σ-type molecular orbital made up mainly of the in-plane p orbital of the endocyclic nitrogen atom, Fig. 6) can interact with the low-lying d_{z^2} orbital, which is strongly raised in energy.

In the molecular adduct **7** two orbitals (labelled HOMO1 and HOMO2 in Fig. 5) are found roughly at the same energy. These orbitals, largely due to the $3d_{z^2}$ and $3d_{x^2-y^2}$ ao's of the Ni

Table 3 Selected bond lengths (Å) and angles (°) of some phosphoro- and phosphonodithioato complexes and of their adducts with pyridine derivatives

	R, R′ [a]	L	Ni–S	Ni–N	S(1)–P–S(2)	S(1)–Ni–S(2)	Ref.
	EtO, EtO	—	2.230, 2.236	—	103.1	88.5	9(*a*)
	EtO, EtO	**I**	2.49, 2.50	2.11	110.4	81.7	15
	EtO, EtO	4-MePy	2.498, 2.488	2.114	110.20	81.30	12(*j*)
	EtO, EtO	**III**	2.491, 2.505	2.103	111.52	81.58	12(*k*)
	BuO, BuO	**I**	2.511	2.116	111.7	81.5	12(*n*)
	BuO, BuO	**IV**	2.509, 2.508	2.091	112.46	81.91	12(*i*)
11	4-MeOPh, EtO	—	2.220, 2.222	—	101.57	88.14	11(*a*)
10	4-MeOPh, MeO	**IV**	2.492, 2.516	2.103	110.91	81.88	[b]
7	4-MeOPh, MeO	**I**	2.494, 2.504	2.125	110.19	81.68	[b]

[a] Substituents in the [R,R′PS$_2$] moiety. [b] Present work.

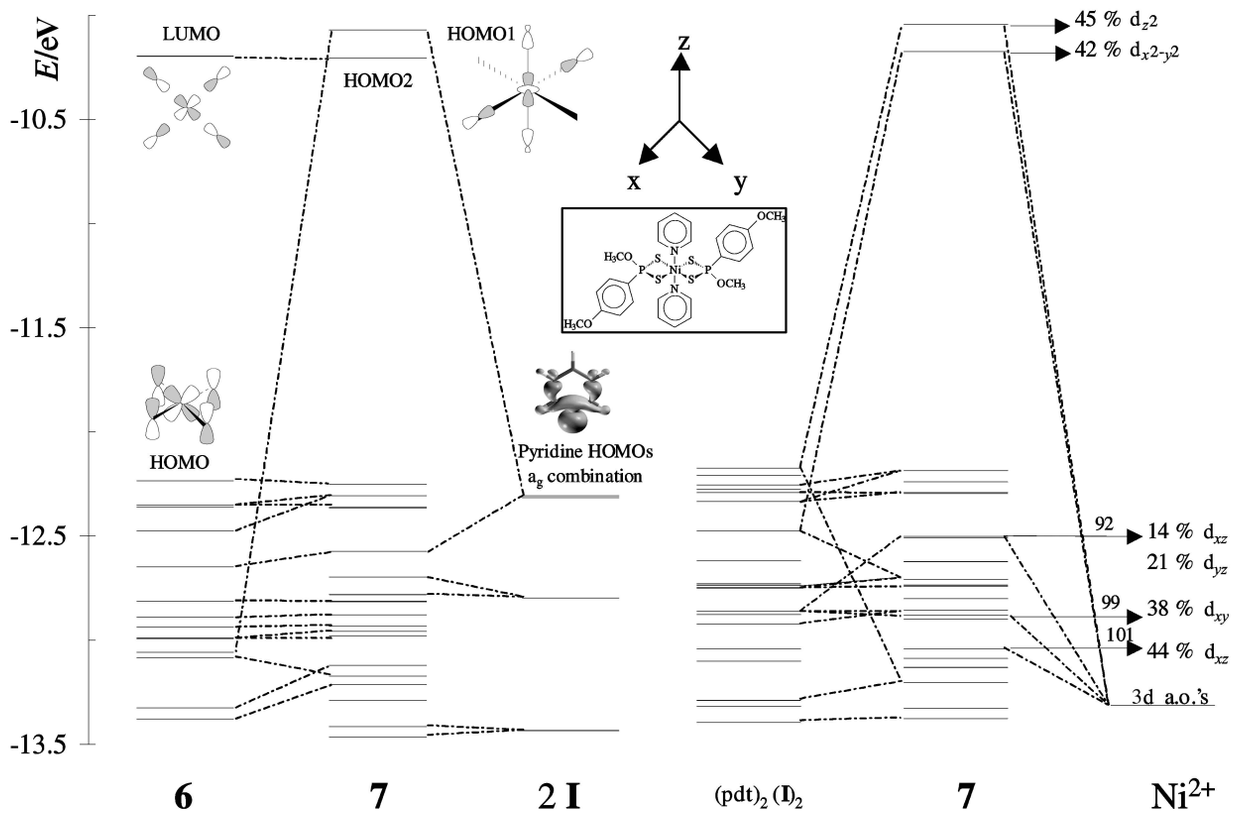

Fig. 5 EHT-FMO diagram of adduct **7** in the range −10.0 to −13.5 eV. On the left side the interaction between complex **6** and the two units of **I** is depicted; the right side shows the interactions of the 3d atomic orbitals of the Ni^{2+} ion with the ligand fragments made up of the phosphonodithioato and pyridine ligands. Dotted lines connect the fragments that contribute to the corresponding molecular orbitals for more than 10%.

atom, host two electrons, causing the paramagnetic behaviour typical in pseudo-octahedral Ni^{II} coordination compounds. In agreement with the Ligand Field Theory point of view, the 3d$_{xy}$, d$_{xz}$, and d$_{yz}$ ao's lie at much lower energies. According to EHT calculations, the LUMO (not shown in Fig. 5) is entirely due to the a$_u$ combination of π-pyridine LUMO's (Fig. 6), made up of an antibonding combination of the carbon and nitrogen atoms and showing two nodal surfaces.

Furthermore, DFT calculations performed on the aminopyridines **II–IV** show that the introduction of an amino group at the pyridine ring dramatically changes the nature of the HOMO's, which become π in nature, and are therefore symmetry-prevented from interacting with the phosphonodithioato complex **6**. Instead the HOMO − 1 orbitals of **II–IV** show the same composition as the pyridine HOMO, and are therefore involved in the adduct formation. Since the Kohn–Sham energies of the HOMO in **I** and those of the HOMO − 1's in **II–IV** are similar, the variation of the donor abilities of the four pyridine derivatives cannot be attributed to energy differences, but more probably to the different charge distribution. In fact, when the amino substituent is found in the *ortho* (**II**) or *para* (**IV**) position the electron pair of the amino group can participate in ring electron delocalisation, causing an increase in electron density at the nitrogen donor atoms (NBO-charges[20] on the endocyclic nitrogen atoms calculated at B3LYP/pVDZ level are −0.236 and −0.219 e for **II** and **IV** respectively, compared with −0.189 e for **I**), while the electron-withdrawing effect of the substituent in the *meta* position causes a slightly opposite effect (NBO-charge −0.186 e for **III**). Therefore, in agreement with the spectrophotometric determinations discussed above, the first two isomers can interact much more efficiently with the phosphonodithioato complex, although steric effects prevent the interaction in the case of the *ortho* isomer.

Conclusions

The reactivity between the phosphonodithioate Ni^{II} complex **6** and the pyridine derivatives **I–IV** has been investigated both in solution and in the solid state. **I–IV** act as donors towards

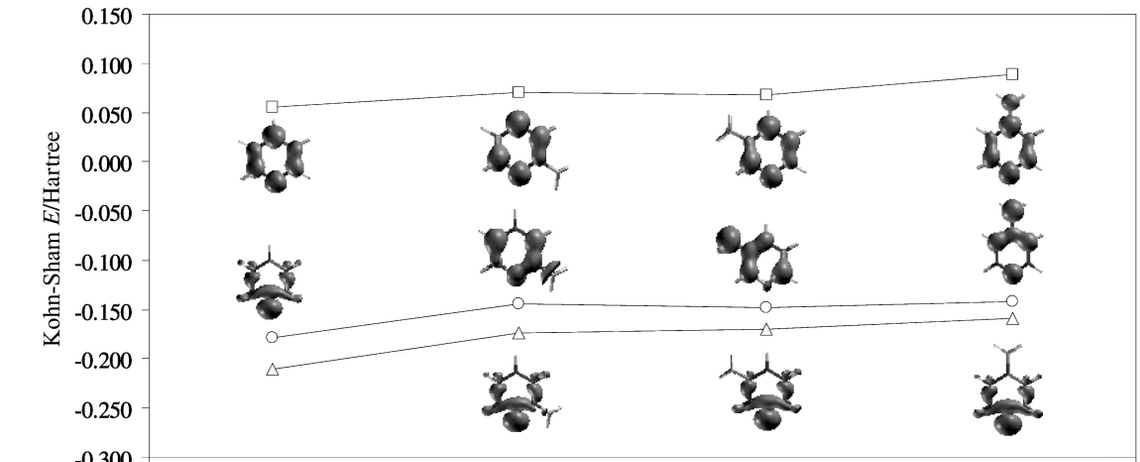

	I	II	III	IV
LUMO	0.056	0.070	0.067	0.089
HOMO	-0.178	-0.144	-0.148	-0.142
HOMO-1	-0.210	-0.174	-0.170	-0.158

Fig. 6 Kohn–Sham energies (Hartree) of the frontier orbitals of pyridine derivatives **I–IV**. (Contour value = 0.05).

the coordinatively unsaturated Ni^{II} ion in **6** and complete its octahedral coordination sphere yielding 1 : 2 adducts which present very similar spectral features. The analyses of the spectrophotometric data confirm that only two species are involved in the equilibrium, thus excluding the formation of complexes having any other stoichiometry. The adduct formation equilibrium constants show that the donor ability increases on passing from **I** to **IV**, in order, except for **II** which exhibits the lowest value in the series. DFT calculations performed on the free ligands show an increase in the electron density at the endocyclic nitrogen atom in the cases of **II** and **IV**, which should correspond to a more efficient interaction with **6**. In fact, FMO-EHT calculations show that the interaction between **I–IV** and **6** mainly involves the Ni d_{z^2} atomic orbital and the HOMO's (HOMO − 1's in the case of **II–IV**) of the two pyridine units, which are made up mainly of the in-plane p orbital of the endocyclic nitrogen atoms. The apparent irregularity in the small value of the formation constant of adduct **8** and the unfeasibility in obtaining this compound in the solid state should be attributed to steric hindrance due to the amino group in the *ortho* position.

Experimental

General

All the reagents and solvents were purchased from Aldrich or Merck, and used without further purification. Elemental analyses were performed with an EA1108 CHNS-O Fisons instrument. Infrared spectra were recorded on a Bruker IFS55 spectrometer at room temperature using a flow of dried air. Far-IR (500–50 cm^{-1}) spectra (resolution 2 cm^{-1}) were recorded as polythene pellets with a Mylar beam-splitter and polythene windows. Mid-IR spectra (resolution 2 cm^{-1}) were recorded as KBr pellets, with a KBr beam-splitter and KBr windows. FT-Raman spectra were recorded as KBr pellets (resolution 2 cm^{-1}) on a Bruker RFS100 FT-Raman spectrometer, fitted with an In–Ga–As detector (room temperature) operating with a Nd–YAG laser (excitation wavelength 1064 nm) with a 180° scattering geometry. The excitation power was modulated between 100 and 250 mW. The UV-visible measurements were performed on a Varian Cary 5 UV-Vis-NIR spectrophotometer equipped with a temperature controller accessory and connected to an IBM PS/2 computer. The spectrophotometric titrations were carried out by adding increasing amounts of a CH_3OH solution of the pyridine ligands to a CH_2Cl_2 solution of **6**,‡ up to complete formation of the adduct. Several spectra were recorded in the range between 400–1100 nm at 25 °C, after each ligand addition. The spectra collected for each ligand were analysed using the program SPECFIT,[15] which automatically corrects the spectra for dilution effects. Factor analysis performed on the set of spectra recorded for each equilibrium afforded the following eigenvalues: **7**: 3.11×10^2, 13.9, 7.92×10^{-3}; **8**: 3.63×10^2, 9.39, 1.53×10^{-2}; **9**: 3.66×10^2, 18.2, 6.52×10^{-3}; **10**: 2.23×10^2, 10.2, 6.07×10^{-3}, confirming the presence of only two species involved in the formation equilibrium. Preliminary values for the formation constants (β_{eq}) of equilibrium (1) have been estimated from the distribution curves. Starting from these estimates, we calculated the β_{eq} values for all the equilibria using a least-squares procedure on the same set of spectra from which the distribution curves were computed. The concentration of the reagents during the titrations, the spectra collected, and the calculated data are available as ESI.†

Syntheses

***trans*-Bis[*O*-methyl-(4-methoxyphenyl)phosphonodithioato]-nickel {[$Ni(pdt)_2$], 6}.** Complex **6** was synthesised according to the previously reported procedure.[11]

[$Ni(pdt)_2py_2$], 7. A quantitative amount of the adduct **7** was obtained as green crystals by slow evaporation of a pyridine solution of complex **6** (0.26 g; 0.5 mmol), mp 145 °C with decomposition, found (calc. for $C_{26}H_{30}N_2O_4P_2S_4Ni$): C, 46.1 (45.7); H, 4.6 (4.4); N, 4.2 (4.1); S, 18.7 (18.8 %). FT-IR (3500–100 cm^{-1}): 3015vw, 2964vw, 2938w, 2837w, 1908vw, 1590vs, 1564s, 1494s, 1451ms, 1438vs, 1403m, 1344w, 1304m, 1294s, 1251vs, 1208ms, 1175s, 1146mw, 1112vs, 1067m, 1037m, 1011vs, 826ms, 792ms, 771vs, 755s, 717w, 694vs, 658vs, 648vs, 625s, 545vs, 520ms, 437ms, 371mw, 349mw, 311w, 242m, 221mw, 199ms, 193mw, 189mw cm^{-1}. FT-Raman (3500–50 cm^{-1}; relative intensities in parentheses related to the highest

‡ Due to solubility reasons, the titrations were performed in a mixture of CH_3OH and CH_2Cl_2 with a v/v ratio which varies during the titration from 0 to 0.4. The values of the formation constants were calculated only on the variation of the spectral shape, and checks were made to verify that the the spectral features of **6** and **7**–**10** do not change on passing from a CH_2Cl_2 solution to a CH_2Cl_2/CH_3OH = 1/0.4 v/v mixture.

Table 4 Summary of X-ray single crystal data and structure refinement parameters for compounds **7** and **10**

Compound	**7**	**10**
Formula	$NiS_4P_2N_2O_4C_{26}H_{30}$	$NiS_4P_2N_4O_4C_{26}H_{32}$
M	683.43	713.45
Crystal system	triclinic	triclinic
Space group	$P\bar{1}$	$P\bar{1}$
a/Å	6.944(2)	10.266(5)
b/Å	9.295(2)	10.992(5)
c/Å	12.503(3)	8.302(4)
α/°	75.70(2)	85.410(4)
β/°	76.59(3)	73.060(5)
γ/°	82.95(3)	64.180(3)
V/Å^3	758.8(4)	805(1)
Z	1	1
T/K	293(2)	293(2)
D_c/g cm^{-3}	1.496	1.471
F(000)	354	370
Crystal size/mm	0.15 × 0.12 × 0.20	0.26 × 0.27 × 0.37
Wavelength/Å	0.71073 (Mo-Kα)	1.54184 (Cu-Kα)
μ/cm^{-1}	10.55	45.52
Transmission factors	1.00–0.90	1.00–0.75
Collected reflections, unique	2696	2964
Observed reflections	1809 [$I > 2\sigma(I)$]	2149 [$I > 2\sigma(I)$]
Final R indices [$I > 2\sigma(I)$]	$R1 = 0.0360$, $wR2 = 0.0852$	$R1 = 0.0405$, $wR2 = 0.1079$
R indices (all data)	$R1 = 0.0726$, $wR2 = 0.0943$	$R1 = 0.0578$, $wR2 = 0.1167$

$R1 = \Sigma||F_o| - |F_c||/\Sigma |F_o|$, $wR2 = [\Sigma[w (F_o^2 - F_c^2)^2]/\Sigma [w (F_o^2)^2]]^{1/2}$.

peak taken equal to 10.0): 3082 (3.6), 2939 (1.4), 2840 (1.4), 1592 (3.8), 1117 (3.5), 1012 (2.5), 802 (1.6), 640 (1.6), 552 (6.2), 313 (3.3), 187 (2.3), 114 (5.6), 83 (10.0) cm^{-1}.

[Ni(pdt)$_2$(*m*-NH$_2$py)$_2$], 9. An excess of **III** (0.53 g; 5.6 mmol) in MeOH was added dropwise to a solution of **6** (0.26 g; 0.5 mmol) in 50 mL of CH_2Cl_2. The adduct was obtained as green crystals by slow evaporation of the solution at room temperature, but it could not be isolated from the solution because it was unstable. As soon as the solution is removed, the adduct decomposes losing the pyridine ligands, even under inert atmosphere.

[Ni(pdt)$_2$(*p*-NH$_2$py)$_2$], 10. An excess of **IV** (0.28 g; 2.9 mmol) in MeOH was added dropwise to a solution of **6** (0.08 g; 0.15 mmol) in 10 mL of CH_2Cl_2. The adduct was quantitatively obtained as green crystals by slow evaporation of the solution at room temperature, mp 159 °C, found (calc. for $C_{26}H_{32}N_4O_4P_2S_4Ni$): C, 44.0 (43.7); H, 4.6 (4.8); N, 7.9 (7.8); S, 17.9 (17.9%). FT-IR (3500–100 cm^{-1}): 3450s, 3359vs, 3335ms, 3086vw, 3053vw, 2981w, 2936w, 1911w, 1638vs, 1618s, 1591s, 1571m, 1559mw, 1497s, 1467mw, 1445m, 1403w, 1384w, 1360vw, 1346w, 1341w, 1304w, 1288mw, 1276w, 1252s, 1212ms, 1185ms, 1114s, 1056w, 1030vs, 1013s, 948vw, 852w, 830s, 823s, 800ms, 771s, 735vw, 716vw, 671ms, 663ms, 649s, 626ms, 545s, 441m, 370w, 349w, 311w cm^{-1}. FT-Raman (3500–50 cm^{-1}; relative intensities in parentheses related to the highest peak taken equal to 10.0): 3062 (3.5), 3055 (3.9), 1588 (2.4), 1183 (0.9), 1112 (3.5), 1056 (1.0), 1011 (2.1), 854 (3.1), 666 (0.8), 546 (3.5), 295 (1.1), 118 (5.2), 95.4 (4.9), 83 (10.0), 75.2 (7.0) cm^{-1}.

X-Ray crystal structure determination. Crystallographic and experimental details of the data collection and refinement of the structures of **7** and **10** are reported in Table 4. The intensity data were collected at room temperature on a CAD 4 single crystal diffractometer, using graphite monochromated Mo-Kα radiation (0.71073 Å) for **7** ($\omega/2\theta$ scan technique), and graphite monochromated Cu-Kα radiation (1.54184 Å) for **10** ($\theta/2\theta$ scans technique), respectively. Data were corrected for Lorentz and polarisation effects as well as for absorption.[21] Both structures were solved by Patterson and Fourier methods and refined by full-matrix least-squares procedures (based on F_o^2) with anisotropic thermal parameters in the last cycles of refinement for all the non-hydrogen atoms. The hydrogen atoms were introduced into the geometrically calculated positions and refined riding on the corresponding carbon atoms for **7**, whereas they were refined with no constraints for compound **10**. All calculations were carried out using the SHELXS-97 program.[22]

CCDC reference numbers 157796 and 157797.

See http://www.rsc.org/suppdata/dt/b1/b100991p/ for crystallographic data in CIF or other electronic format.

Gaussian 94 output files for **I–IV** are available on request from the author.

Computations. The qualitative MO analysis of **7** was obtained by means of the Extended Hückel Theory (EHT)[19] using the CACAO (Computer Aided Composition of Atomic Orbitals) program package[23] at the experimental geometry. The interaction diagrams were generated using the fragment molecular orbital (FMO) approach.[18] Parameters used in EHT calculations were taken from the standard database of CACAO. The NBO-charges[20] on the endocyclic nitrogen atoms in compounds **I–IV** were calculated with the commercially available Gaussian 94 package,[24] at Density Functional Theory (DFT) optimised geometries.[25] The Becke3LYP hybrid functional (which uses a mixture[26] of Hartree–Fock and DFT exchange along with DFT correlation: Lee–Yang–Parr correlation functional[27] together with Becke's gradient correction),[28] and Schafer, Horn and Ahlrichs pVDZ basis sets[29] were used throughout. Integration was performed numerically using a total of 7500 points for each atom (Finegrid option). The Kohn–Sham orbitals were analysed by means of the Molden 3.6 program.[30]

References

1 J. R. Wasson, G. M. Woltermann and H. J. Stoklosa, *Fortschr. Chem. Forsch. (Top. Curr. Chem.)*, 1973, **35**, 65.

2 W. Kuchen and H. Hertel, *Angew. Chem., Int. Ed. Engl.*, 1969, **8**, 89.

3 P. G. Harrison, M. J. Begley, T. Kikabhai and F. Killer, *J. Chem. Soc., Dalton Trans.*, 1986, 925; Y. Lin, *Lubr. Eng.*, 1995, **51**(10), 855; A. J. Burn, I. Gosney, C. P. Warrens and J. P. Wastle, *J. Chem. Soc., Perkin Trans. 2*, 1995, 265; J. M. Georges, A. Tonck, S. Paoletti, E. S. Yamaguchi and P. R. Ryason, *Tribol. Trans.*, 1998, **41**(4), 543; S. Contarini, G. Tripaldi, G. Ponti, S. Lizzit, A. Baraldi and G. Paolucci, *Appl. Surf. Sci.*, 1997, **108**(3), 359; B. Chen, J. Song, Y. Ye and J. Dong, *Tribologia*, 1998, **29**(2), 207.

4 M. D. Sexton, *J. Chem. Soc., Perkin Trans. 2*, 1984, 1771.
5 H. So, Y. C. Lin, G. S. Huang Gibbs and S. T. Chang Terny, *Wear*, 1993, **166**, 17; V. V. Mikhailov, Yu V. Kokhanov, K. Kazaryan, E. N. Matreeva and A. Kozodoi, *Plast. Massy*, 1970, **9**, 23; M. Fuller, M. Kasrai, J. S. Sheasby, G. M. Bancroft, K. Fyfe and K. H. Tan, *Tribol. Lett.*, 1995, 367.
6 R. C. Mehrotra, G. Srivastava and B. P. S. Chauhan, *Coord. Chem. Rev.*, 1984, **55**, 207 and refs. 2–6 therein.
7 R. B. Fearing, E. N. Walsh, J. J. Menn and A. H. Freiberg, *J. Agric. Food Chem.*, 1969, **17**(6), 1261; D. A. Wustner, J. Desmarchelier and T. R. Fukuto, *Life Sci.*, 1972, **11**(11), 583; Y. Miyata, Y. Takahashi and H. Ando, *Kagaku. Keiatsu. Kenkyusho Hokoku., Hokagaku-hen*, 1988, **41**(2), 159; N. K. Roy, *Pesticides*, 1990, 13.
8 R. Engel, *Chem. Rev.*, 1976, **77**, 349; K. H. Scheidt, in *Nucleotide Analogues*, Wiley & Sons, New York, 1980, pp. 96–141; R. Engel, in *The Role of Phosphonates in Living Systems*, ed. R. L. Hildebrand, CRC Press, Boca Raton, FL, 1983, pp. 93–138; G. M. Blackburn and D. E. Kent, *J. Chem. Soc., Perkin Trans. 1*, 1986, 913; G. R. J. Thatcher and A. S. Campbell, *J. Org. Chem.*, 1993, **58**, 2272; M. de F. Fernandez, C. P. Vlaar, H. Fan, Y.-H. Liu, F. R. Fronczek and R. P. Hammer, *J. Org. Chem.*, 1995, **60**, 7390; I. Kers, J. Stawinsky and A. Kraszewsky, *Tetrahedron Lett.*, 1998, **39**(10), 1219.
9 (*a*) V. Kastalsky and J. F. McConnell, *Acta Crystallogr.*, 1967, **22**, 853 For some reviews on these compounds see; (*b*) I. Haiduc, *Rev. Inorg. Chem.*, 1981, **3**, 353; (*c*) I. Haiduc, D. B. Sowerby and S.-F. Lu, *Polyhedron*, 1995, **14**, 3389; (*d*) I. Haiduc and D. B. Sowerby, *Polyhedron*, 1996, **15**, 2469.
10 L. Malatesta and R. Pizzotti, *Chim. Ind. (Milan)*, 1945, **27**, 6; L. Malatesta and R. Pizzotti, *Gazz. Chim. Ital.*, 1946, **76**, 167; P. S. Shetty, P. Jose and Q. Fernando, *J. Chem. Soc.*, 1968, 788; H. Hartung, *Z. Chem.*, 1967, **7**, 241; J. P. Fackler, Jr. and L. D. Thompson, Jr., *Inorg. Chim. Acta*, 1981, **48**, 45.
11 (*a*) M. Arca, A. Cornia, F. A. Devillanova, A. C. Fabretti, F. Isaia, V. Lippolis and G. Verani, *Inorg. Chim. Acta*, 1997, **262**, 81; (*b*) M. C. Aragoni, M. Arca, F. Demartin, F. A. Devillanova, C. Graiff, F. Isaia, V. Lippolis, A. Tiripicchio and G. Verani, *Eur. J. Inorg. Chem.*, 2000, 2239.
12 (*a*) H. W. Chen and J. P. Fackler, *Am. Cryst. Assoc. Summer Meeting.*, 1974, 229; S. X. Liu, C. C. Lin, Y. P. Yu, D. L. Zhu, Z. Xu, S. H. Gou and X. Z. You, *Acta Crystallogr., Sect. C*, 1991, **47**, 43; S. Ooi and Q. Fernando, *Inorg. Chem.*, 1967, **6**, 1558; S. X. Liu, C. C. Lin, Z. Xu, Y. P. Yu and X. Z. You, *Youji Huaxue (J. Org. Chem.)*, 1987, 369; S. X. Liu, X. C. Lin, Z. Xu, J. H. Lin, Y. P. Yu and X. Z. You, *Gaodeng Xuexiao Huaxue Xuebao*, 1989, **10**, 1225; *Chem. Abstr.*, 1990, **113**, 47494f; X. Z. You, Z. Xu, X. Xu, J. H. Lin, Y. P. Yu, C. C. Lin and S. X. Liu, *Kexue Tongbao (Chin. Sci. Bull.)*, 1992, **37**, 657; *Chem. Abstr.*, 1993, **118**, 110525n; S. K. Arora, D. E. Carter, Q. Fernando and K. Seff, *Acta Crystallogr., Sect. B*, 1977, **33**, 3230; X. Z. You, Z. Xu, Y. P. Yu, S. X. Liu and C. C. Lin, *Jiegou Hauxue (J. Struct. Chem.)*, 1986, **5**, 154; *Chem. Abstr.*, 1987, **107**, 124911v; M. Shiro and Q. Fernando, *J. Chem. Soc. D*, 1971, 350; D. C. Craig, E. T. Pallister and N. C. Stephenson, *Acta Crystallogr., Sect. B*, 1971, **27**, 1163; D. B. Sowerby and I. Haiduc, *Inorg. Chim. Acta*, 1976, **17**, L15; D. B. Sowerby and I. Haiduc, *Inorg. Nucl. Chem. Lett.*, 1976, **12**, 791; (*b*) P. S. Shetty and Q. Fernando, *J. Am. Chem. Soc.*, 1970, **92**, 3964; P. Porta, A. Sgamelotti and N. Vinciguerra, *Inorg. Chem.*, 1971, **10**, 541; (*c*) R. Micu-Semeniuc, L. Silaghi-Dumitrescu and I. Haiduc, *Inorg. Chim. Acta*, 1976, **17**, 5; (*d*) R. Constantinescu and I. Haiduc, *Inorg. Chim. Acta*, 1976, **19**, 105; (*e*) R. Micu-Semeniuc, L. Silaghi-Dumitrescu, N. Chirila and I. Haiduc, *Rev. Roum. Chim.*, 1980, **25**, 1025; (*f*) R. Micu-Semeniuc, O. Cristina and I. Haiduc, *Rev. Roum. Chim.*, 1980, **25**, 1489; (*g*) C. P. Bhasin, G. Srivastava and R. C. Mehrotra, *Inorg. Chim. Acta*, 1983, **77**, L131; (*h*) R. Micu-Semeniuc, L. Silaghi-Dumitrescu and I. Haiduc, *Synth. React. Inorg. Met.-Org. Chem.*, 1993, **23**(10), 1629; (*i*) J.-X. Dong, X.-Y. Huang, X.-Z. You and R.-G. Xiong, *Polyhedron*, 1994, **13**(19), 2763; (*j*) B.-L. Song, R.-G. Xiong, X.-Y. Huang and X.-Z. You, *Acta Crystallogr. Sect. C.*, 1995, **51**, 2258; (*k*) R.-G. Xiong, X.-Z. You and X.-Y. Huang, *Acta Crystallogr., Sect. C*, 1995, **51**, 2261; (*l*) R.-G. Xiong, X.-Y. Huang and X.-Z. You, *Acta Crystallogr., Sect. C*, 1995, **51**, 2263; (*m*) J. S. Huang, Y. P. You, Z. Xu and X. X. You, *Acta Crystallogr., Sect. C*, 1990, **46**, 991; (*n*) S. X. Liu, C. C. Lin, Z. Xu, Y. P. Yu and X. Z. You, *Youji Huaxue (J. Org. Chem.)*, 1987, **5**, 369.
13 M. Shiomi, M. Tokashik, H. Tomizawa and T. Kuribayashi, *Lubr. Sci.*, 1989, **1**, 131; M. W. Sulek, *Tribologia*, 1993, **24**, 67.
14 H. Gampp, M. Maeder, Ch. J. Meyer and A. D. Zuberbuhler, *Talanta*, 1985, **32**, 1133; H. Gampp, M. Maeder, Ch. J. Meyer and A. D. Zuberbuhler, *Talanta*, 1986, **33**, 943; H. Gampp, M. Maeder, Ch. J. Meyer and A. D. Zuberbuhler, *Anal. Chim. Acta.*, 1987, **193**, 287.
15 M. C. Aragoni, M. Casu, F. Cesare Marincola, G. Crisponi, M. Casu, F. Cristiani and V. M. Nurchi, *Ann. Chim. (Rome)*, 1999, **89**, 167.
16 S. Ooi and Q. Fernando, *Inorg. Chem.*, 1967, **6**(8), 1558.
17 M. Chao and E. Schempp, *Acta Crystallogr., Sect. B*, 1977, **33**, 1557 and refs. therein.
18 H. Fujimoto and R. J. Hoffmann, *Phys. Chem.*, 1974, **78**, 1167.
19 R. Hoffmann and W. N. Libscomb, *J. Chem. Phys.*, 1962, **36**, 2179.
20 A. E. Reed, L. A. Curtiss and F. Weinholt, *Chem. Rev.*, 1988, **88**, 899.
21 N. Walker and D. Stuart, *Acta Crystallogr., Sect. A*, 1983, **39**, 158; F. Ugozzoli, *Comput. Chem.*, 1987, **11**, 109; A. C. T. North, D. C. Phillips and F. S. Mathews, *Acta Crystallogr., Sect. A*, 1968, **24**, 351.
22 G. M. Sheldrick, SHELXS-97, Program for the solution and the refinement of crystal structures, University of Göttingen, Germany, 1997.
23 C. Mealli and D. M. Proserpio, *J. Chem. Educ.*, 1990, **67**, 399.
24 Gaussian 94 (Revisions D.1 & E.1), M. J. Frisch, G. W. Trucks, H. B. Schlegel, P. M. W. Gill, B. G. Johnson, M. A. Robb, J. R. Cheeseman, T. A. Keith, G. A. Petersson, J. A. Montgomery, K. Raghavachari, M. A. Al-Laham, V. G. Zakrzewski, J. V. Ortiz, J. B. Foresman, C. Y. Peng, P. Y. Ayala, M. W. Wong, J. L. Andres, E. S. Replogle, R. Gomperts, R. L. Martin, D. J. Fox, J. S. Binkley, D. J. Defrees, J. Baker, J. P. Stewart, M. Head-Gordon, C. Gonzalez and J. A. Pople, Gaussian, Inc., Pittsburgh PA, 1995.
25 J. Labanowsky and J. Andzelm, *Density Functional Methods in Chemistry*, Springer-Verlag, New York, 1991.
26 A. D. Becke, *J. Chem. Phys.*, 1993, **98**, 1372.
27 C. Lee, W. Yang and R. G. Parr, *Phys. Rev. B*, 1998, **37**, 785.
28 A. D. Becke, *J. Chem. Phys.*, 1993, **98**, 5648.
29 A. Schafer, H. Horn and R. Ahlrichs, *J. Chem. Phys.*, 1992, **97**, 2571.
30 G. Schaftenaar and J. H. Noordik, *J. Comput.-Aided Mol. Des.*, 2000, **14**, 123.